The Experimental Studies on the EOR Effects of Air Injection Displacement in the Low Permeable Reservoirs

Jian Luan[a,b], Pingchuan Dong[a,b,] * , Jilong Zheng[c,d]

[a]State Key Laboratory of Petroleum Resources and Prospecting, China University of Petroleum (Beijing), Beijing 102249, China

[b]College of Petroleum Engineering, China University of Petroleum (Beijing), Beijing 102249, China

[c]CNOOC EnerTech-Drilling & Production Co，Tianjin 300452，China;

[d]State Key Laboratory of Offshore Oilfield Exploitation，Tianjin 300452，China

A B S T R A C T

The low permeable oil reservoirs account for a large proportion of the total number of oil reservoirs in the world and the number of them surpass half of the total number of the oil reservoirs in China, it is important to exploit this kind of reservoir effectively. The water flooding exploitive results of these reservoir are usually very poor because of the tiny pores, bad pore connections and so on. However, these problems can be well solved by applying gas injection techniques, especially air injection. In this paper, the EOR effects of the injection parameters such as oxygen content in the injected air, the injection speed etc. were studied by several experiments using independently designed equipments aiming at one low permeable sandstone reservoir in China.

Several conclusions were made from the experiment results: the best recovery effects can be achieved by injecting the deoxygenated air with 8% of O_2 using the methods of injecting the air slugs and the foaming agent slugs alternately etc.. At last, several formulae about relationships between the EOR and the air injection parameters were revealed. These formulae may offer some references to the air injection process mechanisms studies of the similar oil reservoir.

Keywards:

Low permeable oil reservoir

Air injection

EOR

* Corresponding author
E-mail address: dpcfem@163.com(P. C. Dong)

Dynamic Experiments

Formulae

1 Introduction

With the development of the petroleum industry, rarely the oil reservoirs with good geological conditions were left after nearly 200 years exploration and exploitation. However, abundant oil and gas resources were still trapped in the oil and gas reservoirs which with inferior initial conditions, among which, a large part of this kind of resources are accounted for by reservoirs with the permeability lower than 50 mD. In China, the oil and gas in place trapped in this kind of reservoirs is over half of the proved reserves. Up till the beginning of 2013, the proved reserves in the reservoirs with low permeability in China was over 53.7×10^8t, which accounted for 49% of the total reserves and over 65% of the newly proved reserves every year was trapped in this kind of reservoirs[1-4]. In the world, the oil in the low permeable reservoirs accounts for more than 65% of the newly proved reserves each year. According to the reasons above, the reservoirs with low permeability will be the prime objectives of the oil and gas exploration and exploitation in the future. What's more, it is of vital importance to exploit them effectively to relief the domestic and world pressure of the energy demands[5-8].

The properties of the reservoirs with low permeabilities are relatively very bad, the pores and the throats are very small, the anisotropy, heterogeneity and the complicated degree of the reservoir structures are very strong, the initial productivity of the oil reservoir usually very low and it usually decreases quite fast. These are all the disadvantages of the depletive methods to exploit the low permeable oil reservoirs. What's more, it is very difficult to exploit them by using water drive methods because the severe problems of water sensitivity, water lock, and speed sensitivity will be easily caused. The unified recognitions of the microscopic geological reasons that cause the unsteady production and the low recovery factor have not been achieved. Besides these, the problems such as the big starting pressure in the producing process, the uneven distribution of the formation pressure, the significant differences of the production profiles, the vast existence of the non-linear flow, the low productivities of the well and the fast rising of the water content in the produces liquid after water breakthrough will cause the unsatisfactory water flooding consequences. The low water flooding recovery factors, the abundant of the residual oil in the formation and the

poor simulative accuracy of the seepage models are all the shortcomings of water flooding methods[9-13]. However, technologies such as gas injections, especially high pressure air injection (HPAI) can increase the injectivity of the displacing media, solve the problems of water lock, water sensitivity etc. and have been recognized as the effective methods to exploit the reservoirs with low permeability [14, 15].

The technologies of air injection are a new kind of safe, environment protective and effective EOR technologies with broad prospects which were developed within recent decades. They represent a brand new kind of EOR methods with increasing application trends on matter in sandstone oil reservoirs or carbonate reservoirs [16, 17]. The oil was oxidized spontaneously by the air injected into the oil reservoir under high pressure in the process of this kind of technologies. The flue gas which was mainly composed by CO_2 and N_2 was generated at the same time when the components of the oil and the injected air were changed. After mixing with the other gas in the reservoir, the flue gas and other gas will form the gas mixture that will act as the main force to drive the oil [18-23].

2 The EOR mechanisms and Some Problems of air injection in Oil Reservoirs

2.1 EOR mechanisms

2.1.1 Low Temperature Oxidation Reactions

After the air was injected into the oil reservoirs, the oxygen in the injected air will react with the components in the oil under or a little higher than the temperature of the reservoir and cause the physical and chemical changes of the components in the oil and gas phases, these kinds of spontaneously occurred reactions are usually called Low Temperature Oxidation (LTO). In the processes of LTO, the oil components will be involved in the dehydrogenation reactions and oxygenation reactions. As a result, lots of water, CO_2, and the derivatives of the hydrocarbon such as ketones, aldehydes and ethers will be produced. The main processes are shown in Fig. 1[24-26].

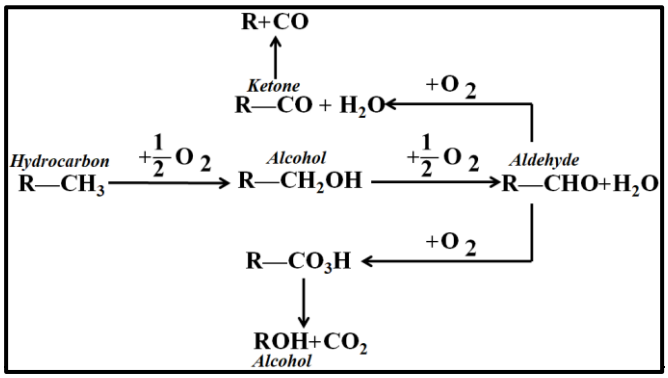

Fig. 1. The mechanisms of LTO of oil and oxygen in the injected air

2.1.2 The Flue Gas Flooding

It can be concluded from Fig. 1 that after the air was injected into the reservoir, the media in the reservoir to displace the oil is the flue gas composed by the CO, CO_2, N_2 and other evaporative light hydrocarbon components which are generated by the oxidation reactions between the oil and oxygen in the injected air. The degree of the LTO reactions depends on the pressure, temperature, the components of the oil, water, gas, minerals and the oxygen concentration in the injected air. Finally, the flue gas will displace the oil, this process combines the mechanisms of increasing the sweep coefficient, decreasing the surface tension and miscible flooding, finally, the effects of EOR can be achieved[27-29].

2.1.3 Air-Foam Flooding

Because the viscosity of the air in the air injection technology is much lower than that of the oil, which means the injected gas will gather at the top of the reservoir. What's more, the adverse mobility ratio will be generated (M>1) because of the flowability of the gas is much better than that of the oil, which means as the flooding processes goes on, many adverse phenomena such as fingering, gas channeling and gravity overlap will be generated and leave many dead oil zones in the reservoirs. Hence, the recovery factor will be reduced severely and even creat some pathways with high permeabilities connecting the injection wells and the production wells. What's worse, these non-piston flooding phenomena will more severe if the reservoir contains fractures or different layers with large permeability differences.

In order to solve the problems of fast channeling of the injected gas in the reservoir, foam was always employed as a disperse system to control the channeling of the gas. Up till now, two methods of foaming were used in the oil field: one is to foam on the surface on the ground and another is to foam in the reservoir underground. Because the foam created on the ground will

broken and be defoamed because of the shear in the process of the injection, the methods of foaming underground in the reservoir are more efficient. During the process of injecting foam, the gas and the foaming agents slugs were injected into the reservoir alternatingly, the foam will be created when the gas passes through the porous media, such as rock, into the already injected foaming agents. Sometimes, polymer gel is injected along with the foaming agents in order to increase the foam abilities of blocking and prevent the gas channeling[30-32].

Overall, the mechanisms of foam flooding are as follows:

(1) Gas resistance effects

The injected water firstly enter the larger pores according to the Darcy's Law and drive the oil in them out in the water flooding processes and this will cause lots of residual oil was left in the smaller pores in the unflooded area. The flow speed of the fluid in the bigger pores is slower than that in the smaller pores, which will cause the shearing rates in the bigger pores are smaller than those in the smaller pores. This will make the foam viscosity in the larger pores larger than that in the smaller pores because of the non-newtonian and pseudoplastic fluid characteristics of the foam. Consequently, the foam will enter the smaller pores of the unflooded area first and achieve the goal of adjusting the water adsorption profiles, hence, the macroscopic sweeping coefficient E_V will be enhanced.

(2) Ameliorate the mobility ratio

Due to the larger apparent viscosity of the foam in the larger pores, it can achieve the effects of polymer flooding to some extent, which can increase the viscosity of the injected fluid, reduce its flowability and adjust the water adsorption profiles. Finally, the fingering and non-piston flooding phenomena will be reduced and the recovery factor can be enhanced.

(3) Increase the sweeping coefficient

The resistances of foam seeping in the formation include internal friction of the liquid phase, the resistance caused by the collision of the liquid droplets with the gas and the resistances caused by Jamin effects due to the shrinks of the seeping tunnels. At this time, the flow resistance will be increased by the existence of the foam and the flooding in the high permeable layers will be slowed down, then the flooding effects in the low permeable layers can be increased.

(4) Enhance the microscopic flooding efficiency

Due to the long contacting time of the oil and the formation rock, the surface of the formation

will be changed into oil-wet surface. What's more, the adsorption extent of the oil on the rock surface can be increased by the heterogeneity of the reservoir. However, the foaming agents in the injected foam system is a good kind of surfactant, the wettability of the rock surface can be largely ameliorated by the unique amphiphilic molecular structure of the foaming agents molecules. The surface of the reservoir rock can be turned from oil wetting into water wetting by this kind of molecular, and then, the adsorbed oil can be easily washed down. What's more, the oil film on the surface of the reservoir rock can be stripped away through emulsification effects. Finally, the microscopic driving efficiency E_D can be improved.

(5) Selective blockage

Due to the bizarre foam system characters: stable when mixed with water and defoam when mixed with oil, when the foam is injected into the formation, it will exist stably at the parts where are thoroughly water flooded and with higher water saturation. At these parts of the reservoir, the blockage effects of the foam system can be well exerted. While at the high oil saturated parts of the reservoir, the foams will break spontaneously. These will relatively reduce the resistance of water flooding in the unflooded area of the reservoir and make it easier for the displacing fluid to enter the unflooded parts of the reservoir. Finally, the goals of ameliorating the water adsorption profiles can be achieved[33-42].

2.2 Existing Problems

There are still several problems in applying the air injection techniques in the low permeabile oil reservoir:

1. Little references about the applicabilities and the results about applying the air injection technologies in this kind of reservoirs could be found.
2. Further studies about the parameters about the air injection processes in this kind of reservoirs are still needed.
3. There are no references about the relationships about the recovery factor and the parameters of air injection process.
4. The methods of injecting air are still needed to be optimized.

The problems above are still to be studied and solved via some experiments in this study.

3 The Dynamic Oxidation and Flooding Experiments of the Oil

3.1 Oil Reservoir Characteristics

The target reservoir of this study is an offshore oil reservoir in China. which area is over 115km^2. Up till now, the average pressure of the reservoir is 23MPa, the temperature ranges from 90℃ to 110℃. The rock permeability is less than 40mD, so it is a low permeable oil reservoir. The exploitative results of water flooding were very bad, however, if the depletive methods are employed, the reservoir will witness a quick pressure dropdown, the sweeping area will be restrained within a narrow area around the injector. Finally, a big amount of residual oil will be left in the formation and the final recovery factor will be very low. Due to the reasons above, the air injection technologies are selected to exploit this low permeable oil reservoir.

3.2 Experimental Equipment

The self-designed isothermal sand packing flooding system was used in the experiments, the flow chart is shown in Fig. 2. Among the equipments, the inner length of the sand packed tube is 100cm, the inner diameter is 38mm, its pressure limit is over 60MPa. The temperature limit of the isothermal incubator is over 300℃; the pressure limit of the high pressure pump is over 90MPa. The pipes connect each equipment are made from hastelloy alloy with 4 mm outer diameter and pressure limits over 40MPa. The temperature limit of the pressure-temperature sensors is more than 300℃ and the pressure limit of the back-pressure valve is over 35 MPa. All the equipments can fulfill the demands of the experiments.

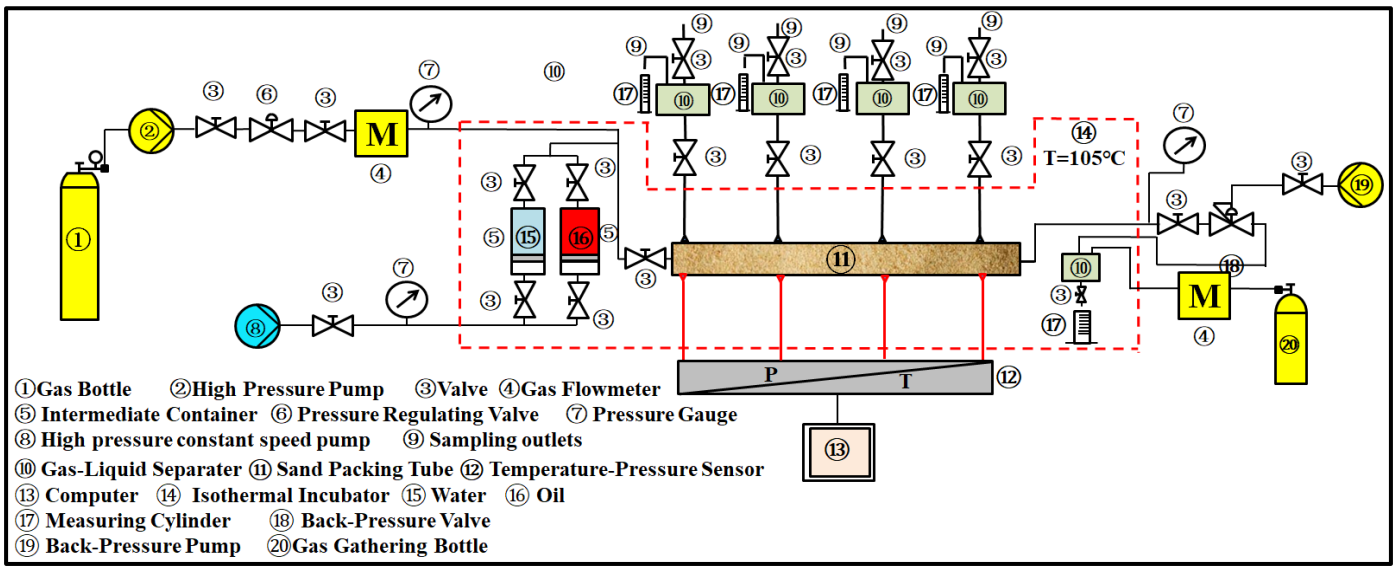

Fig. 2. The flow chart of the experimental equipment

All kinds of the fluid, including formation water and oil samples used in the experiments are

sampled from the production sites of the target reservoir. The wax concentration of the oil is relatively high, which ranges from 25% to 36%, so the oil viscosity is sensitive to the change of the temperature, the relationship of oil viscosity and the temperature are shown in Fig. 3. From 10℃ to 200 ℃, the viscosity decreases dramatically as the temperature rises due to the high content of the wax, from over 3600 mPa · s in 10℃ to less than 0.1 mPa · s in 200℃, and when the temperature is over 500℃, the viscosity levels out around 0.005 mPa · s. As for the reservoir condition, the oil viscosity changes within the range from 0.98 mPa · s to 1.15 mPa · s.

The components and their concentration in the formation oil were measured by means of chromatography analyses, as are shown in Fig. 4. In Fig. 4, every saturated hydrocarbon is represented by the letter "C" and the number of carbon atoms in their molecules for short.

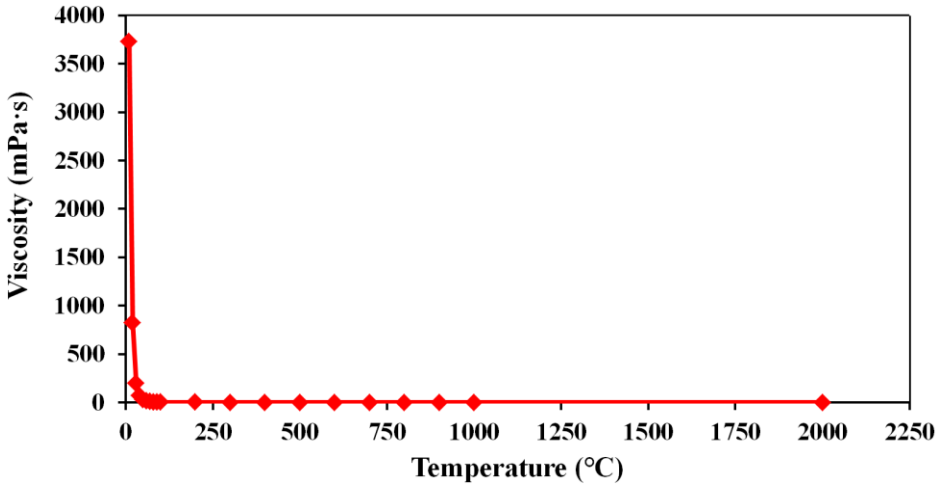

Fig. 3. The viscosity-temperature relationship curve of the oil sample

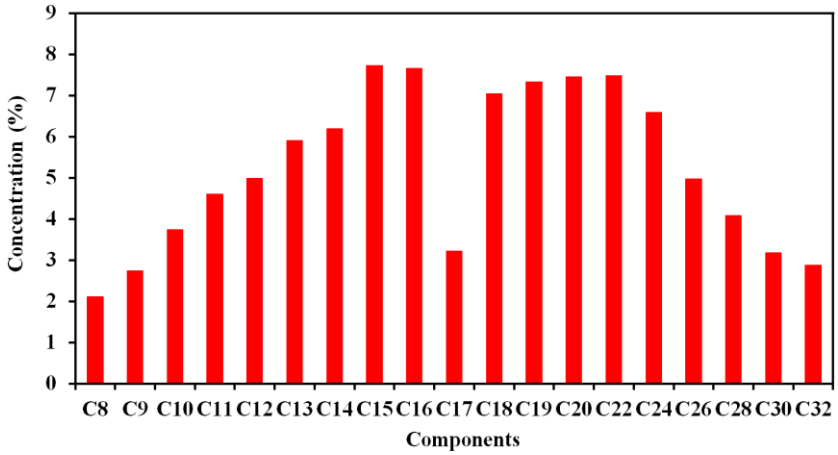

Fig. 4. The components and content of the oil sample

3.3 Experimental Procedures

3.3.1 Optimization of the Oxygen Concentration in the Injected Air

The oil, injected water samples from the target oil reservoir and the deoxygenated air which are common used in the oil field (the oxygen concentration are 8%, 10%, 21% and pure nitrogen) were used to carry out the displacement experiments in order to select the best oxygen concentration. The injected air are bought from a gas corporation which provide gas for the oil field.

Four displacement experiments were carried out using the equipment depicted in the Fig. 2. In every experiment, one kind of the deoxygenated air mentioned above was used to displace the oil in the sand packed tube. The procedures are as follows:

1. Tightly packed the tube with 2kg formation sand and then measured the porosity and permeability after the formation water was saturated into the tube.
2. Connected the tube with other equipments, as are shown in Fig. 2, saturated it with formation water under the experimental condition (23MPa and 105℃) and then saturated it with oil sample.
3. The ageing processes were simulated by leaving the tube in the isothermal incubator for 24 hours.
4. Set the back-pressure valve pressure at 23MPa, the flooding processes were carried out with the water injection velocity of 2ml/min under the experiment condition (23MPa ,105℃) until the out flow fluid water cut was over 98%.
5. The gas flooding procedures were carried out by injecting the deoxygenated air with different oxygen concentration(8%、10%、21% and nitrogen) using high-pressure pump at the speed of 0.3 ml/min until on liquid was driven out at the outlets of the equipment.
6. The ageing process of the tube was repeated for another 12 hours in the isothermal incubator after it was flooded by gas.
7. The secondary water flooding after gas flooding and gas–water alternated flooding processes were simulated by injecting water at the constant speed (2ml/min) until the the produced liquid water cut was over 98%, then the chromatography analysis were done.
8. The best oxygen concentration was optimized via comparing the recovery factor of each experiment in order to continue the experiments.

3.3.2 Oxidation Time Optimization

The experiments were carried out using the equipment shown in Fig. 2, the first four steps were the same as those in the first group of experiment.

The optimized deoxygenated air was injected into the tube until the pressure was built up to

23MPa and let the oil reacted with the deoxygenated air for 30 days, the liquid and gas samples were got every other 12 hours during the experiment to carry out the chromatographic analyses.

3.3.3 Injection Rate Optimization

The experiments were carried out using the equipments shown in Fig. 2, the first four steps were the same as those in the first group of experiment.

Inject the deoxygenated air at different rate such as 0.02ml/min, 0.05ml/min, 0.1ml/min, 0.15ml/min, 0.2ml/min, 0.3ml/min, 0.4ml/min and 0.5ml/min under the experimental condition by adjusting the valve, the optimized injection rate was got by analyzing the final recovery factor.

3.3.4 Crude Oil LTO under Different Temperature Studies

Four groups of experiments were carried out, the first four steps were the same as those of the first experiment, the only differences are the experimental temperatures were set as 95℃, 105℃, 110℃ and 120℃ respectively.

The optimized deoxygenated air was injected to drive the oil under the condition of 23MPa until no liquid was produced from the outlets. The differences between the LTO reactions under different temperatures were got by comparing the concentration changes of the components.

3.3.5 Different Injection Methods Optimization

3.3.5.1 Gas–Water Alternated Flooding Methods

The first four steps of the first groups of experiments were repeated.

Then, the gas flooding processes were simulated by injecting the optimized deoxygenated air under the optimized injecting rate until no liquid was produced at the outlets.

The tube was rested in the incubator to simulate the aging processes for 12 hours.

Secondary water flooding was carried out under the same condition until the liquid water cut from the outlets was over 98% and then the chromatography analyses were carried out. The recovery factor of each stage were calculated by measuring the oil volume.

3.3.5.2 Air-Foam Flooding Methods

The first four steps were the same as the first experiment.

Underground foaming processes were simulated by injecting 0.03PV of foaming agents solution after 0.03PV of the selected deoxygenated air slug was injected into the tube. Then, foam slugs were generated in the tube to drive the oil, these processes were repeated until the injected fluid

breakthrough at the outlets.

The aging processes were conducted by leaving the tube in the incubator for 12 hours.

The processes of water flooding after foam injection was conducted by injecting water at the speed of 2 ml/min until the water cut of the produced liquid was over 98%.

3.3.6 The effects of the Reservoir Heterogeneity

The formation heterogeneity effects on the dynamic oil oxidation were studied in this group of experiments. According to the permeability ratio definition: $J_K = \frac{K_{MAX}}{K_{MIN}}$, three groups of experiments were carried out in order to study the heterogeneity effects on the oil oxidation under the circumstances of J_k is 2, 3, and 5. In each experiment, two parallelly connected sand packed tubes were flooded simultaneously, all the experimental equipments and flow chart are shown in Fig. 5.

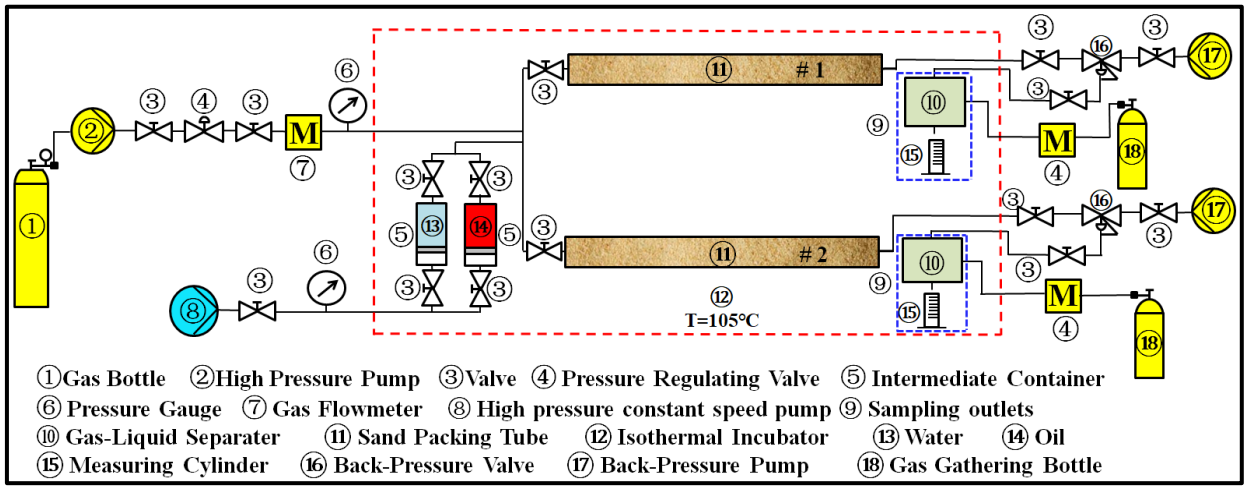

Fig. 5. The flow chart of the experimental equipments

The first four steps of the first experiment were repeated.

The foaming agents and the optimized deoxygenated air were injected in the best methods to carry out the foam flooding until the injected fluid breakthrough at the outlets.

Formation water was injected at a constant rate until the produced fluid water cut at the outlets was over 98% to simulate secondary water flooding, then some chromatographic analyses were carried out. The reservoir heterogeneity effects were analyzed by comparing the recovery factor of each group of experiments.

4 Experimental Results Analyses

4.1 Oxygen Concentration Optimization Results

The sand packed tube properties in each experiment were shown in Table 1.

Table 1 Sand Packed Tube Properties

O_2 Concentration （%）	Pore Volume （ml）	Oil Volume （ml）	Water Volume （ml）	Oil Saturation （%）	Prosity （%）	Permeability （mD）
0	395	333	62	84	34.90	46.76
8	405	340	65	84.0	35.73	47.87
10	412	330	82	80	36.30	47.37
21	402	360	42	90	35.5	46.78

The relationships of the total injected air PV and the total EOR and the EOR of the injected air are depicted in Fig. 6 and Fig. 7 respectively. According to the results, the air with oxygen concentration of 21% can increase the oil recovery factor by the largest degree, which was more than 10.5% and the total volume of the injected air is the least when the recovery factor came to a stable state. What's more, the reaction rate with oil was the fastest due to the highest oxygen concentration and the rate of EOR was also the most rapid. The EOR extent of air with 8% and 10% oxygen concentration were similar, which were a little less than 10.5%, just a little inferior to that of the air with 21% of oxygen concentration. However, due to the absence of the oxidability, the oxidative reactions cannot occur among the nitrogen and the hydrocarbon components in the oil. The effects achieved by the injected nitrogen were only the supplements of the reservoir energies by volume expansion, so the EOR degree of injecting nitrogen was the lowest.

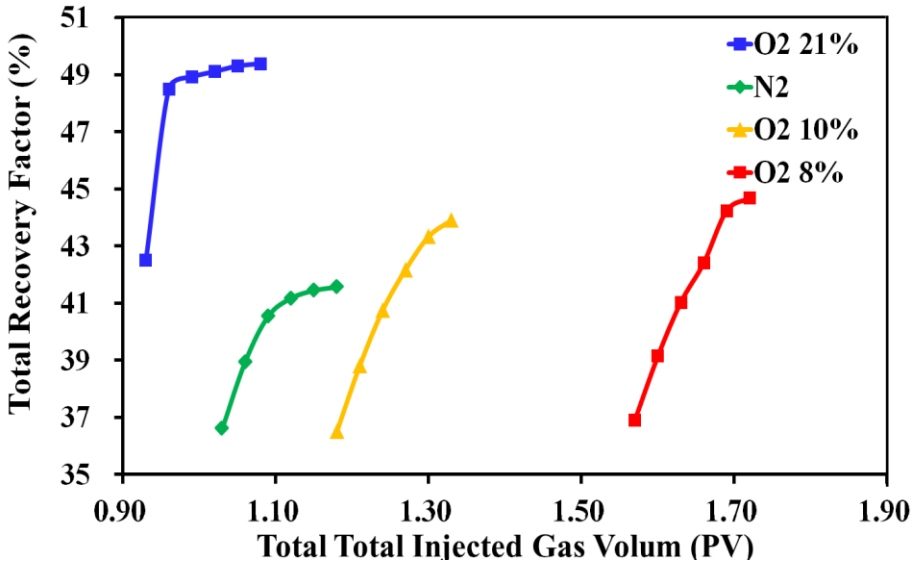

Fig. 6. The total recovery factor versus the total injected gas volume

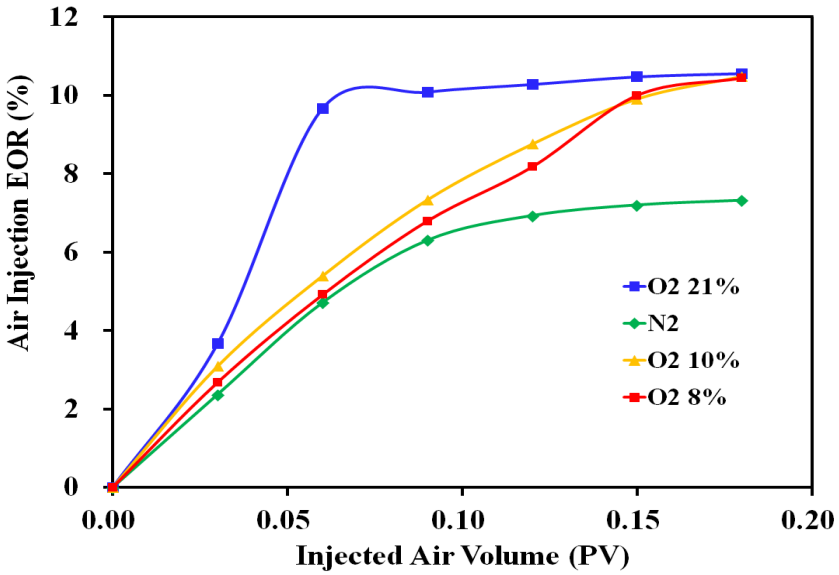

Fig. 7. Air injection EOR versus the total injected gas volume

Fig. 8 shows the recovery factor in each flooding stage. Conclusions can be made that the recovery factor were nearly the same in the first water flooding stage, however, in the air injection stage, the recovery factor rose along with the increase of the oxygen concentration in the injected air. But when the oxygen concentration of the injected air is over 8%, the increase of the recovery factor was not obvious, what's more, in terms of safety of the production, the safety limits of the oxygen concentration on the produced gas in the air injection processes should be less than 9% according to some references[1, 2, 51, 52].

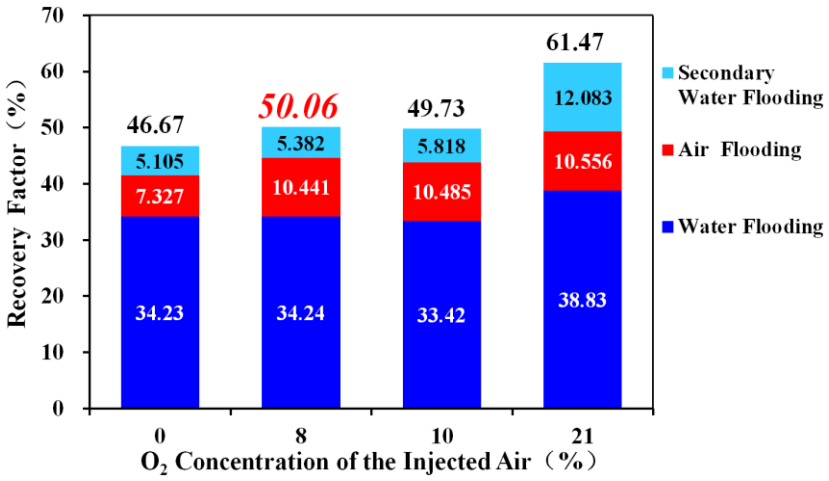

Fig. 8. The different stages EOR of air injection with different oxygen concentration

According to Fig. 8, the recovery factor of each stages rose with the increase of the oxygen concentration in the injected air, however, when the oxygen concentration is over 8%, the recovery factor increased more and more slowly and unnoticeably. Taking the erosion and the oxidation of the pipeline, the equipments and the safety into consideration, the oxygen concentration should be

as low as possible on the premise that the EOR results are nearly the same. So, the optimized oxygen concentration was 8%.

As for nitrogen, because of its absence of oxidative effects to the hydrocarbon, the analyses were mainly focus on the experimental results of the air with 8%, 10% and 21% of oxygen. According to the experiments, the equation about the relationship of the EOR degree, the oxygen concentration in the injected air and the PV of the injected air was derived, as is shown in formula (1):

$$\mathbf{EOR} = \left[\mathbf{6.5073} - \mathbf{0.973}\ln\left(C_{O_2}\right)\right]\ln(\mathbf{V}_{air}) - \mathbf{0.278}\ln\left(C_{O_2}\right) + \mathbf{18.495} \quad (1)$$

Where *EOR* is enhanced oil recovery, %. C_{O_2} is the oxygen concentration in the injected air, %. V_{air} is the total volume of the injected air under surface conditions, PV. *In(x)* is the logarithm function with e as its base.

The comparisons of experimental results and the calculation results of formulae (1) are depicted in Fig. 9, 10 and 11. The comparisons show that most of the calculational results fit the experimental results very well, which means Formula (1) is accurate and reliable.

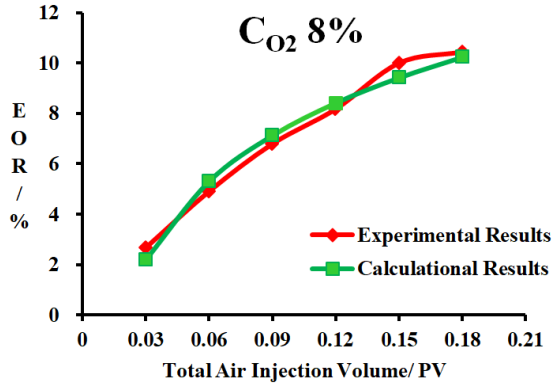

Fig.9 The EOR Experimental and Calculation results Comparison (O2 Concentration 8%)

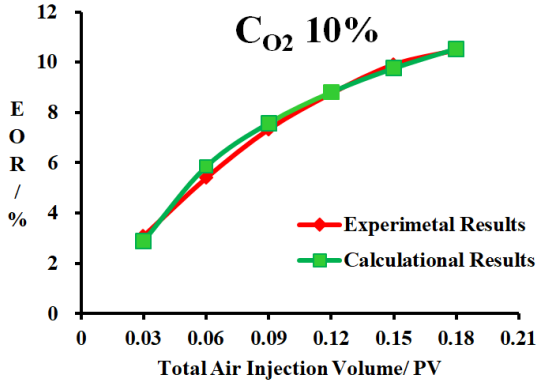

Fig.10 The EOR Experimental and Calculation results Comparison (O2 Concentration 10%)

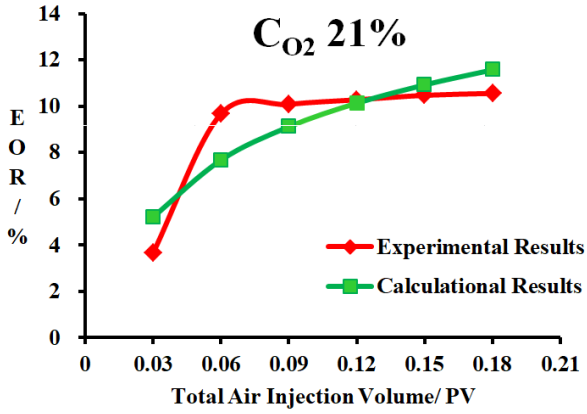

Fig.11 The EOR Experimental and Calculation results Comparison (O2 Concentration 21%)

4.2 Oxidative Reaction Time Optimization Results

The best time of oxidation were got by analyzing the changing trends of the oxygen and CO_2 concentration curve, the oxygen consumption rates of the parts from near to far from the injection point were shown from Fig. 12 to Fig. 16. In these figures, only the curve within the first 168 hours (7 days) of the reaction were depicted because of the stability of the curve after 168 hours(7 days).

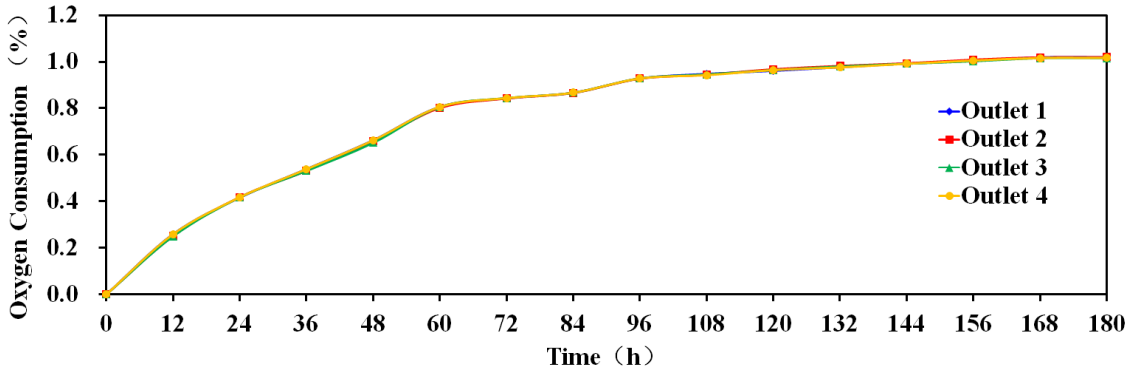

Fig. 12. The oxygen consumption of each outlet

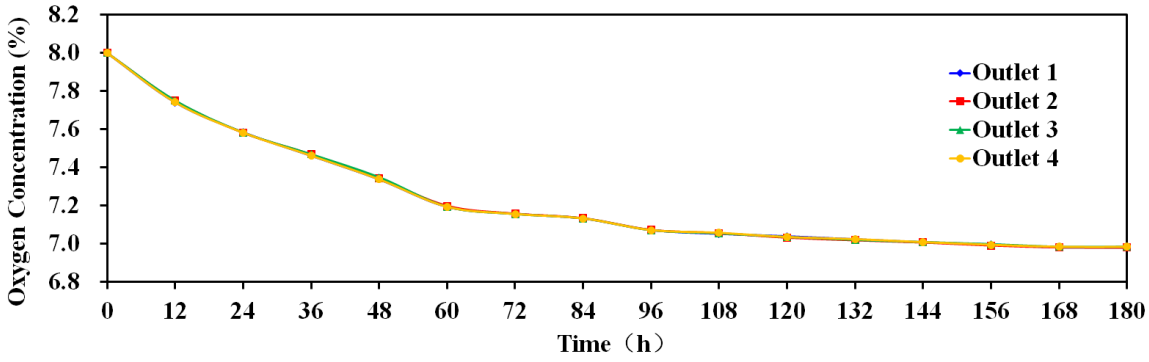

Fig. 13. The oxygen concentration of each outlet

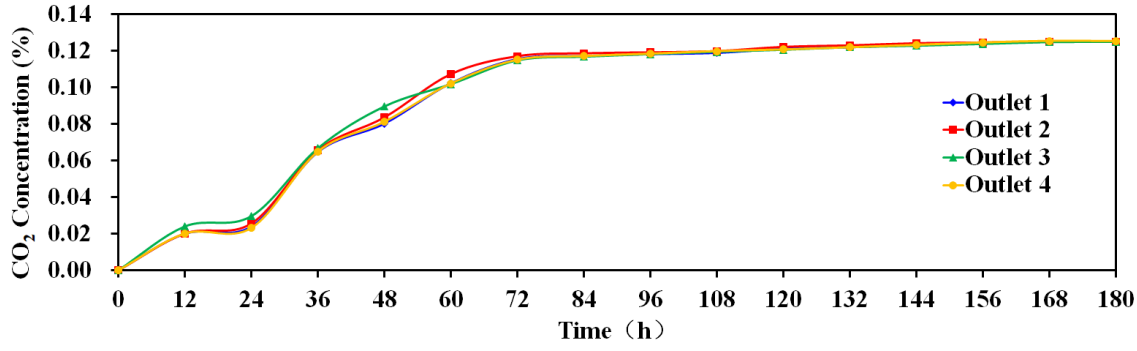

Fig. 14. The CO_2 concentration of each outlet

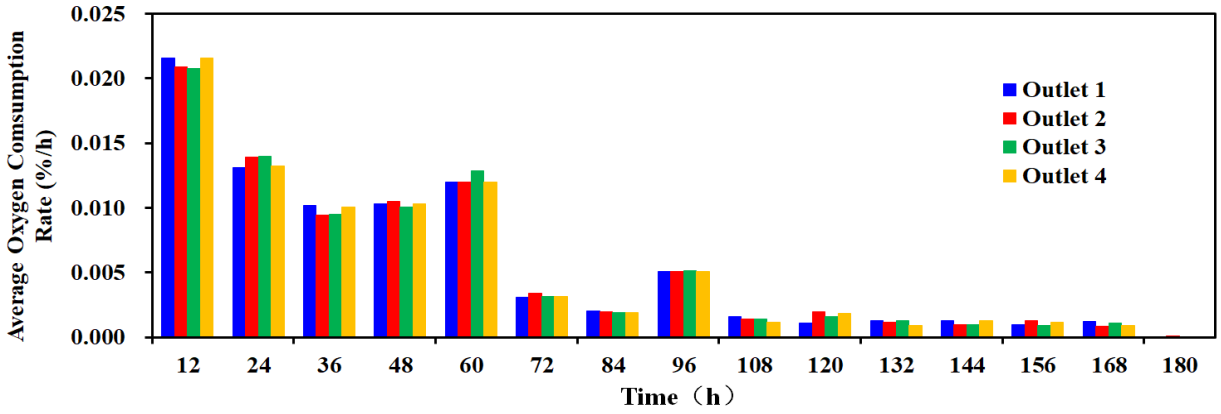

Fig. 15. The average oxygen consumption rate of each outlet

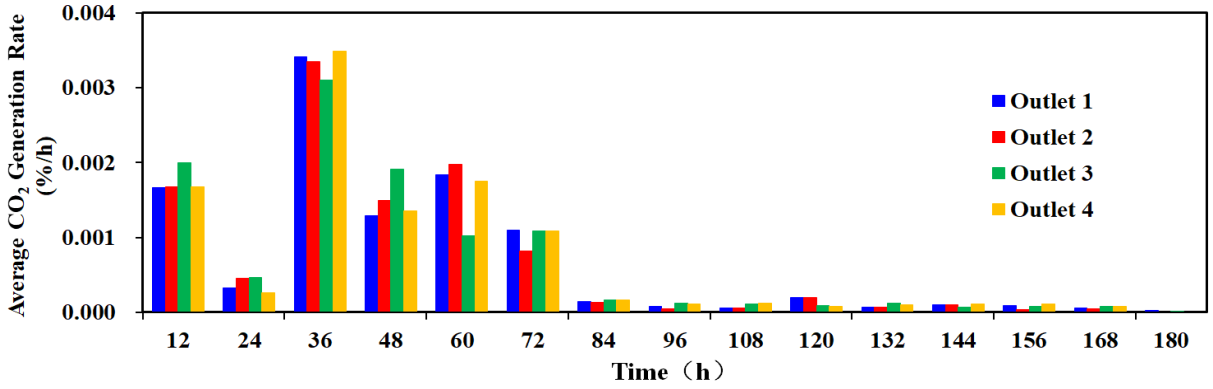

Fig. 16. The average co2 generation rate of each outlet

It can be seen from Fig. 12 to Fig. 16 that with in the first 168 hours (7 days) of the experiments, the consumption of oxygen and the generation of the CO_2 were quite fierce, among which the oxygen concentration decreased for nearly 1% and the CO_2 concentration rose for over 0.12%. These denoted that the oxygen and CO_2 was the mainly gaseous reactant and resultant respectively. After the 168th hour of the experiments, rarely did the concentration of these two kinds of gas change, which can be proved by the Fig. 15 and Fig. 16. In these two figures, the average generation and consumption rate of CO_2 and O_2 are shown. Finally, the best oxidation time of the LTO reactions was determined as the 168 hours (7 days) after the reactions began.

4.3 Oxygen Injection Rate Optimization Results

The original properties of the sand packed tube are shown in Table 2.

The recovery factor of the water flooding, deoxygenated air flooding and secondary water flooding were depicted in Fig. 17. Conclusions can be made that with the increment of the air injection rate, the trend of the recovery factor was increase gradually at first, then followed by a slow drop down. The peak of the recovery factor showed up as 50.06% when the injection rate was

0.3ml/min and the EOR of the air injection was also the largest value: 10.441%. While, when the injection rate exceeded 0.3ml/min, the recovery factor and the EOR of the air injection both demonstrated a decline due to the gas channeling according to the analyses. So, the optimized air injection rate was chosen as 0.3ml/min.

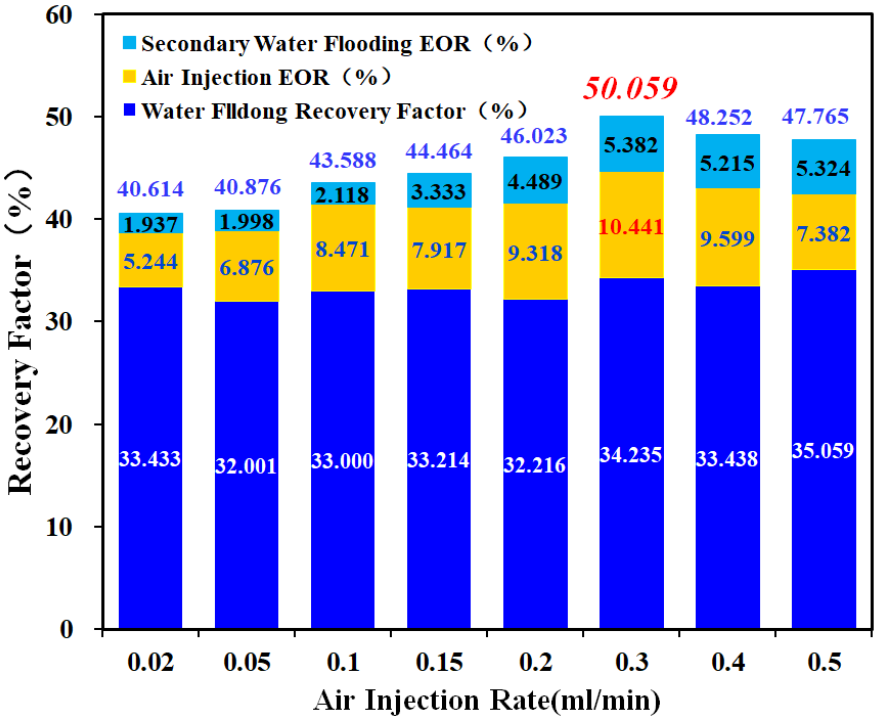

Fig. 17. The Recovery Factor of Different Driving Stage under Different Air Injection Rate

The water cut and recovery factor of the optimized injection rate (0.3ml/min) are depicted in Fig. 18. From Fig. 18, it can be seen that the produced fluid water cut increased rapidly when the at the beginning of the water flooding period (water injected volume $\leqslant$ 0.23PV), then it fluctuated dramatically and rose gradually to more than 99% when the injected water was over 1.54PV. Meanwhile, the recovery factor grew up to 14.09% relatively fast at first when the injected water volume was less than 0.23PV, then followed by a long-term increase to approximate 34.06% slowly when the injected water volume reached 1.34PV and at this moment the water flooding period came to an end. The water injection was ceased when the total water injection volume reached 1.54PV, the air was injected into the tube and the air injection period started. The water cut dropped down dramatically from 99.36% to 21.55% within 0.03PV of injected air. After that, the water cut fluctuated up and down until it reached 85% when the total air injection volume reached 0.3PV and broke through at the outlet, this meant the air injection period ended. During the air injection period,

the recovery factor jumped from 34.24 to 49.12, which meant the air injection method EOR was 14.88. When the secondary water flooding period begun, the water cut rose quickly from 85% to 98.51 after the water was injected 0.13PV and then leveled out around 98.9. The recovery factor increased slightly from 49.12% to 50.06% during this period. Totally speaking, the air injection technique can effectively control the water cut and enhance the recovery factor by 14.08%.

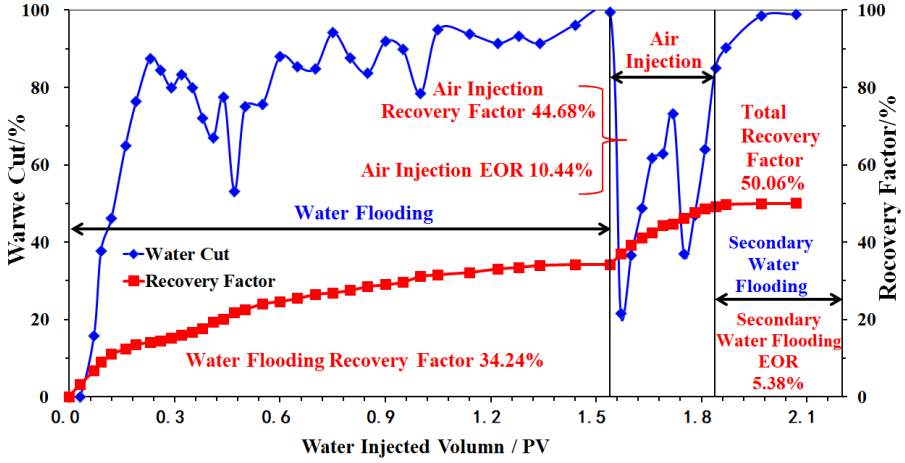

Fig. 18. The Water Cut and Recovery Factor of the Optimized Air Injection Rate Experiment

Table 2 The original properties of the sand packed tube

Gas Injection Rate Gas Injection Rate（ml/min）	Pore Volume（ml）	Oil Volume（ml）	Water Volume（ml）	Oil Saturation（%）	Prosity（%）	Permeability（mD）
0.02	407	336	71	82.555	35.887	47.95
0.05	408	341	67	83.578	35.975	46.75
0.1	410	340	70	82.927	36.152	50.95
0.15	411	336	75	81.752	36.24	40.87
0.2	420	352	68	83.81	37.033	45.94
0.3	405	340	65	83.951	35.711	47.71
0.4	418	349	69	83.493	36.857	42.37
0.5	402	344	58	85.572	35.446	45.57

After the experimental results were studied, some formulae describe the relationships of the EOR and air injection parameters of different condition were brought out, as were shown from formula (2) to formula (7). In order to broaden their application in the oil field, the unit of air injection rate and the total volume of the injected air at surface were converted into PV/min and PV respectively.

$$EOR=(-189665.997833476\Phi^2 R_{air}^2+7096.867232\Phi R_{air}+43.952)\ln(1+V_{air})-7524.32163615$$

$$644\Phi^2 R_{air}^2+72.55109416\Phi R_{air}$$

$$(0\leqslant R_{air}\leqslant 0.00025PV/min,\ 0\leqslant V_{air}\leqslant 0.09\ PV) \quad (2)$$

$$EOR=(-28927.2448291108\Phi^2R_{air}^2+610.5926564\Phi R_{air}+5.8023)\ln(1+V_{air})-32654.77724$$
$$36824\Phi^2 R_{air}^2+756.411242\Phi R_{air}+2.9608$$
$$(0\leqslant R_{air}\leqslant 0.00025PV/min,\ 0.09\ PV<V_{air}\leqslant 0.18\ PV) \quad (3)$$

$$EOR=(929531.712978072R_{air}^2-23959.63498R_{air}+230.83)\ln(1+V_{air})-118.2119897072$$
$$\Phi^2 R_{air}^2+22.3534088\Phi R_{air}$$
$$(0.00025PV/min<R_{air}\leqslant 0.0005PV/min,\ 0\leqslant V_{air}\leqslant 0.09\ PV) \quad (4)$$

$$EOR=(-333010.884482772\Phi^2 R_{air}^2+9435.700314\Phi R_{air}-48.386)\ln(1+V_{air})+103651.356366$$
$$309\Phi^2 R_{air}^2-2752.121766\Phi R_{air}+23.304$$
$$(0.00025PV/min<R_{air}\leqslant 0.0005PV/min,\ 0.09\ PV<V_{air}\leqslant 0.18\ PV) \quad (5)$$

$$EOR=(-15932.92035184\Phi^2 R_{air}^2+847.2531376\Phi R_{air}+67.544)\ln(1+V_{air})-97651.0562097548$$
$$\Phi^3 R_{air}^3+6757.22861599124\Phi^2 R_{air}^2-104.1043136\Phi R_{air}$$
$$(0.0005PV/min<R_{air}\leqslant 0.0013ml/min,\ 0\leqslant V_{air}\leqslant 0.09\ PV) \quad (6)$$

$$EOR=(-73901.767260974\Phi^2 R_{air}^2+3333.17437\Phi R_{air}+11.906)\ln(1+V_{air})+2173.4302238014$$
$$\Phi^2 R_{air}^2-23.294247\Phi R_{air}+1.9784$$
$$(0.0005PV/min<R_{air}\leqslant 0.0013ml/min,\ 0.09\ PV<V_{air}\leqslant 0.18PV) \quad (7)$$

Where Φ is the porosity of the rock, %. R_{air} is the rate of air injection under the surface condition, PV/min. V_{air} is the total volume of injected air at the surface condition.

The Comparisons of EOR experimental results and the calculational results of formulae (2) to formulae (7) are depicted from Fig.19 to Fig. 26. It can be concluded from the comparisons that the calculational results basically match the experimetnal results, which means these formulae are reliable and can be used in the air injection EOR studies.

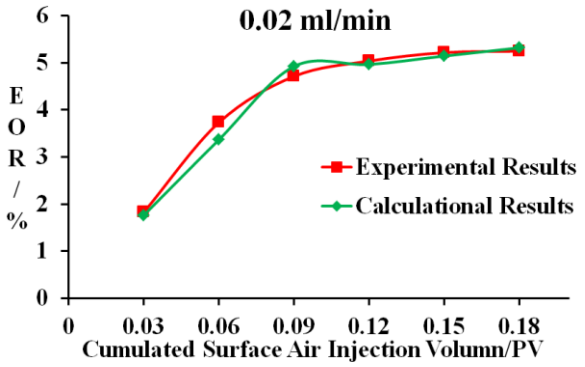

Fig. 19. The EOR Experimental and Calculation Results Comparison (Air Injection Rate 0.02ml/min)

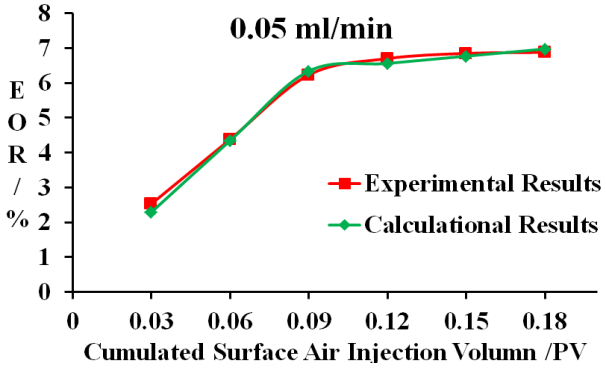

Fig. 20. The EOR Experimental and Calculation Results Comparison (Air Injection Rate 0.05ml/min)

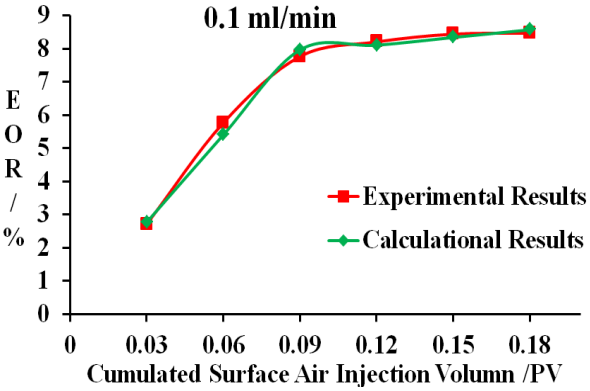

Fig. 21. The EOR Experimental and Calculation Results Comparison (Air Injection Rate 0.1ml/min)

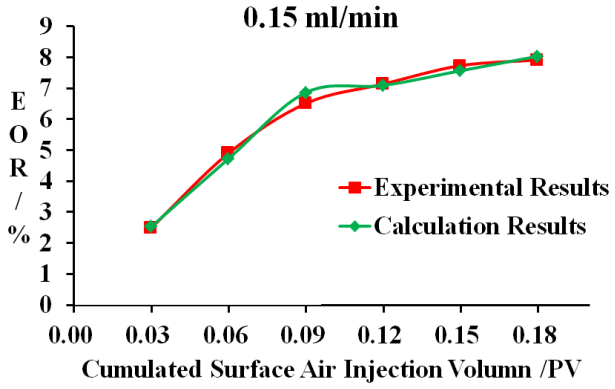

Fig. 22. The EOR Experimental and Calculation Results Comparison (Air Injection Rate 0.15ml/min)

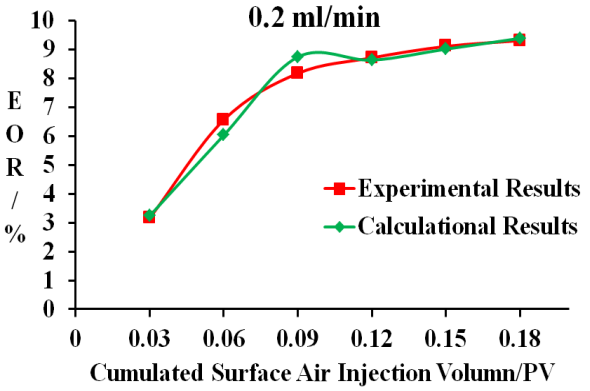

Fig. 23. The EOR Experimental and Calculation Results Comparison (Air Injection Rate 0.2ml/min)

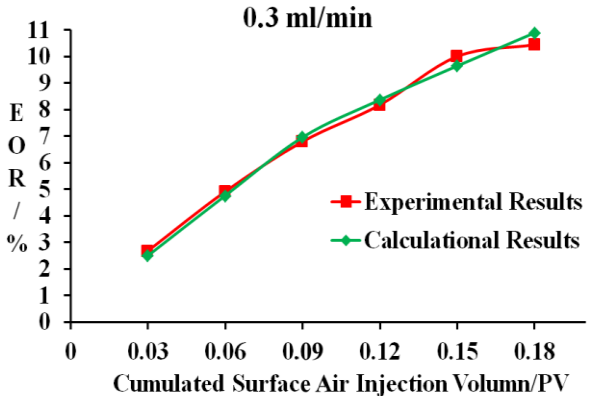

Fig. 24. The EOR Experimental and Calculation Results Comparison (Air Injection Rate 0.3ml/min)

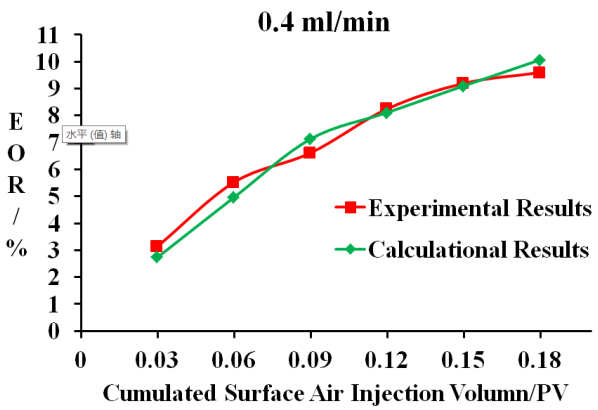

Fig. 25. The EOR Experimental and Calculation Results Comparison (Air Injection Rate 0.4ml/min)

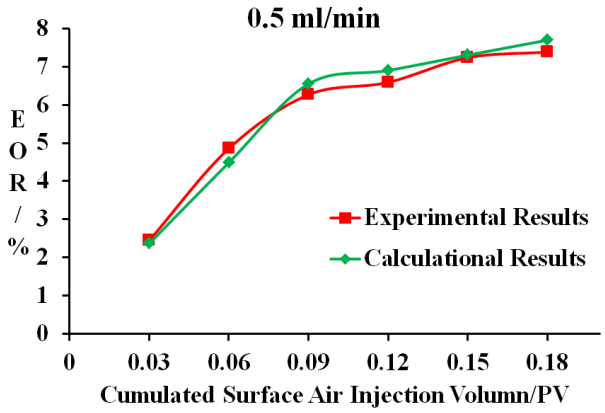

Fig. 26. The EOR Experimental and Calculation Results Comparison (Air Injection Rate 0.5ml/min)

4.4 Oxidation Reaction Under Different Temperature Results

The physical properties of the sand packed tube are listed in Table 3.

Table 3. The original properties of the sand packed tube

Temperature (℃)	PV（ml）	Oil Volume （ml）	Water Volume （ml）	Oil Saturation （%）	Porosity （%）	Permeability （mD）
95	404	342	71	82.555	35.887	47.95
105	405	340	67	83.578	35.975	46.75
110	412	346	70	82.927	36.152	50.95
120	4107	343	75	81.752	36.24	40.87

The total recovery factor and the EOR of air injection in each experiment are depicted and listed in Fig. 27 and Table 4.

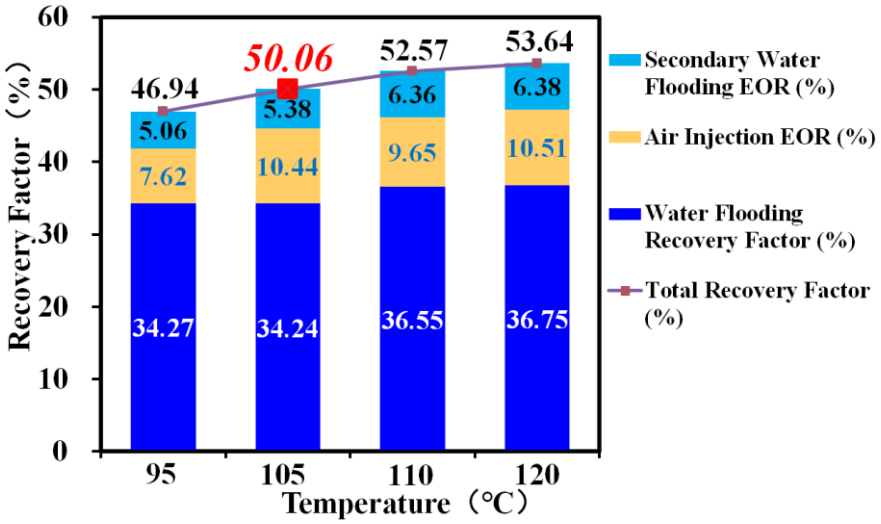

Fig. 27. The water flooding recovery factor, EOR of different flooding stage and Total Recovery Factor of Experiments Under Different Temperature

Table 4. The total racovery factor and the air injection EOR of each experiment

Temperature (℃)	Total Recovery Factor（%）	Air Injection EOR（%）
95	46.94	7.62
105	50.06	10.44
110	52.56	9.65
120	53.63	10.51

Conclusions can be made from Fig. 27 that the total recovery rose with the increment of the temperature, which that the higher the temperature is, the more thoroughly the oxidation of the oil will be. However, as the temperature increase, the increment of the total recovery factor gradually slowed down, which demonstrated that the influences of temperature increment were diminishing. Conclusions can be made from these group of experiments that the oil can be best oxidized under the temperature of 105℃ and the positive correlation relationships between the extent of air injection EOR and the reaction temperature were revealed by this group of experiments.

4.5 Different Injection Methods Optimization Results

The properties of the sand packed tubes in the three groups of experiments are showed in Table 5. In the processes of foam injection, 5 slugs of air and 4 slugs of foaming agents solution whose volume were all 0.03 PV were injected alternatively into the tube to form four foam slugs. According to the results of experimental studies above, deoxygenated air with 8% of oxygen was injected to drive the oil under 23MPa and 105℃ in the methods of water flooding-air foam flooding -secondary water flooding. The recovery factor of each stage were listed in Table 6 and the recovery factor and the EOR of each stage were also depicted in Fig. 28.

Table 5. The original properties of the sand packed tube

Length(cm)	Prosity(%)	Permeability(mD	PV（mL）	Oil Volume（mL）	Water Volume（mL）	S_o(%)
100	35.3	46.1	400	360	40	90

Table 6. The recovery factor and eor of the air foam flooding

	Water Flooding	Air-Foam Flooding	Secondary Water Flooding
Total Recovery Factor（%）	35.56	50.47	62.06
EOR（%）	—	14.91	11.59

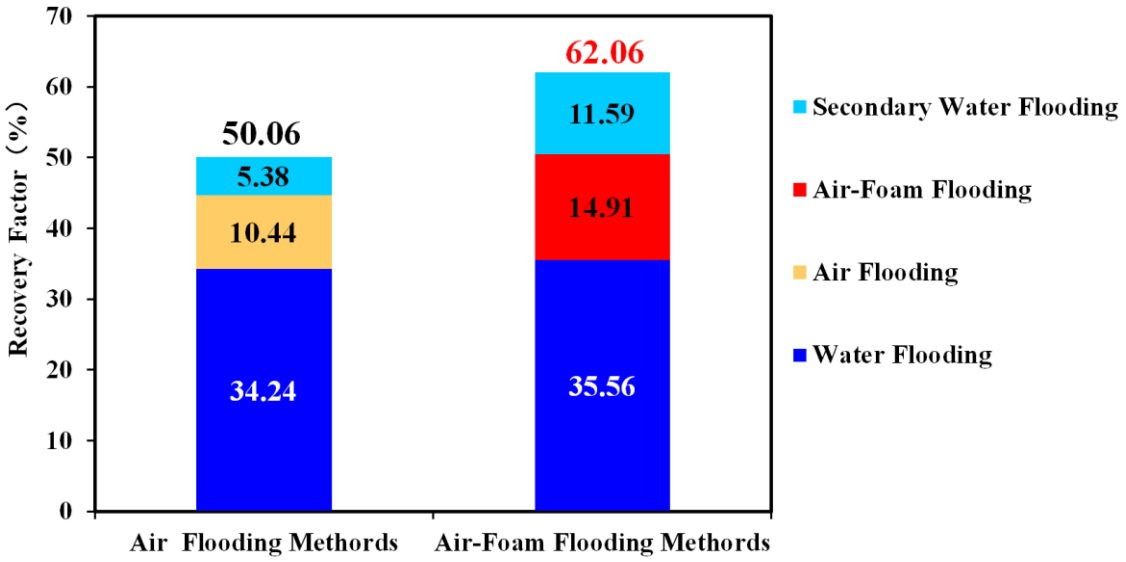

Fig. 28. The recovery factor in each stage of different recovery methods

Conclusions can be made from Table 6 and Fig. 28 that a higher recovery factor can be obtained by applying the air foam injection methods compared to the only usage of air injection methods. The reasons lie in the selective blocking characters of the foam, which means the foam can block the large seepage passages of the water rather than the small seepage passages of oil. So, the seepage passages with larger permeability formed in the early exploitive period can be blocked up and the water adsorption profiles can be adjusted at the same time. What's more, the mobility ratio of the water and the oil can be reduced, the sweep efficiency can be enhanced and the oil in the dead oil zones can be flooded out. Besides these, microscopically speaking, the foaming agents are also a kind of surfactant which can ameliorate the wettability of the formation rock. That's to say, the originally oil-wet rock can be turned into water-wet rock and the oil droplets adsorbed on the surface of the rock can be washed away more easily. These will all result in the increase of the microscopic flooding efficiency E_D. Finally, the recovery factor of the oil can be enhanced macroscopically and microscopically.

Two formulae reveal the relationships of the enhanced oil recovery in the air-foam flooding stage and the parameters of the experiments such as the air injection rate, the volume of the injected fluid and the permeability of the tube were deduced, as are depicted in formula (8) and formula (9):

$$\mathbf{EOR_{air}} = [\frac{3190.81307166231\times\varphi\times \mathbf{R_{air}}}{K(2209.7V_F^3-389.04V_F^2+8.3741V_F+1.1355)}]e^{[(-0.336333E_W)V_F]} \quad (8)$$

$$\mathbf{EOR_{Foam}} = (\frac{961.714092195517\times\varphi\times \mathbf{R_F}}{K})\mathbf{e}^{(-0.098828976\mathbf{E_G})V_F} \quad (9)$$

Where EOR_{air} is the EOR of the injected air slugs in the air-foam flooding stage, %. K is the permeability of the reservoir rock, mD. V_F is the total volume of the injected fluid, PV. E_W is the EOR of the water injection period, %. EOR_{Foam} is the EOR of the injected foaming agents solution slugs in the air-foam flooding stage, %. R_F is the rate of injecting foaming agents solution, PV/min. E_G is the EOR of the gas injection period, %.

The comparisons of air injection and foam injection EOR experimental results and the calculational results of formulae (8) and (9) are depicted in Fig. 29 and Fig. 30 respectively. From the comparison results, it can be seen that the most of calculational results of formulae (8) and (9) can match the experimental results, which means formulae (8) and (9) are reliable.

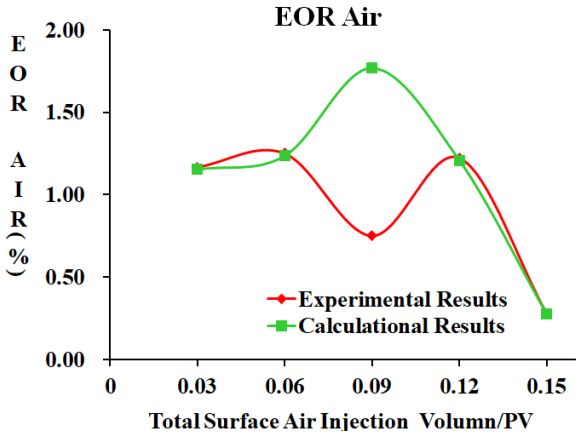

Fig. 29. The Air Injection EOR Experimental and Calculational Results Comparison

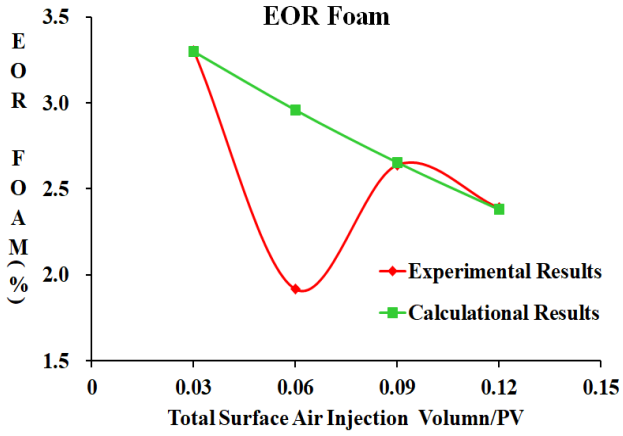

Fig. 30. The Foam EOR Experimental and Calculational Results Comparison

4.6 Formation Heterogeneity Effects Studies Results

The sand packed tube properties in the three groups of the experiments are listed in Table 7.

Table 7. The original properties of the sand packed tubes

J_k	K (mD)	V_p (ml)	V_o (ml)	V_w (ml)	S_o (%)	φ (%)
1:2	49.23	408	343	65	84.06863	35.97519
	102.16	403	345	58	85.60794	35.53432
1:3	46.26	415	363	52	87.46988	36.59241
	158.38	420	362	58	86.19048	37.03328
1:5	48.92	416	363	53	87.25962	36.68059
	243.83	426	336	90	78.87324	37.56233

According to the results above, air with 8% of oxygen was injected in the optimized method to flood the two parallelly connected sand packed tubes, the recovery factor of each tube in the process were depicted in Fig. 31.

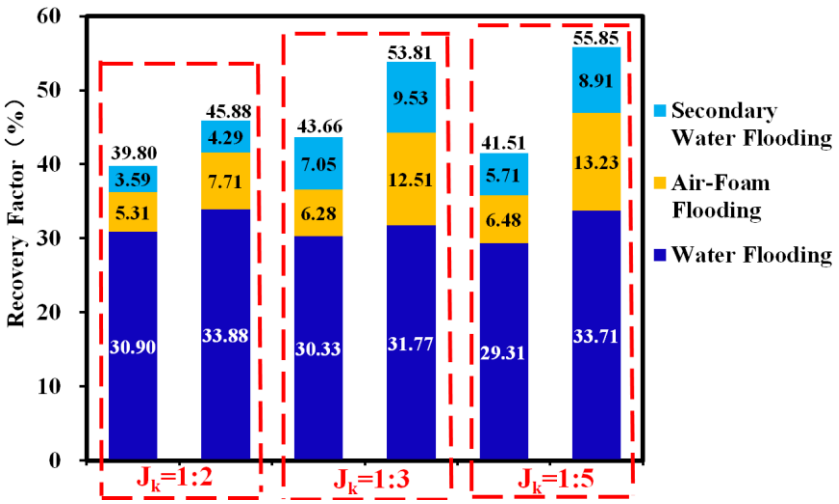

Fig. 31. The recovery factor of each stage of experiments aiming at different permeability ratio

Conclusions can be made according to the Fig. 31 that the total recovery factor of the tube with larger permeability in each experiment is larger than that of the tube with a lower permeability, and so does the EOR of the air-foam flooding. What's more, the larger the permeability ration was, the larger the degree of EOR will be after some EOR measures were taken, especially the tube with larger permeability. The reasons of these phenomena were the flow velocity was small at first in the low permeable tube of the group which has the larger permeability ratio, the oil in the low permeable tube was well preserved and the flow velocity in the other tube in the same group which has a larger permeability was fast and the oil was displaced thoroughly under the same driving pressure difference. While in the air-foam driving processes, oil in the low permeable tube was displaced to a better degree due to the blocking effects of the foam. The larger the permeability ratio was, the better the tube with larger permeability was blocked and the low permeable tube can share a larger displacing pressure difference relatively. According to the Darcy's law, the bigger the pressure difference is, the larger the fluid velocity will be, and the better the oil will be displaced in the tube, finally the better EOR effects can be achieved.

The formulae describing the relationship among the EOR ratio of the two tubes within one group and other parameters in the experiment such as permeability ratio, pressure and the volume of the injected fluid were deduced, which are shown as formulae (10) and (11):

$$\frac{R_{KB}}{R_{KS}} = \frac{\Delta P}{109.2637}\ln(J_K) + 1.1557506\left(\frac{V_{FA}}{V_{FA}+V_{air}}\right) \quad (10)$$

$$\frac{EOR_{KB}}{EOR_{KS}} = \frac{\Delta P}{37.21081}\ln(J_K) + 1.297085\left(\frac{V_{FA}}{V_{FA}+V_{air}}\right) \quad (11)$$

Where R_{KB} is the final recovery factor of the tube with bigger permeability, %. R_{KS} is the final

recovery factor of the tube with smaller permeability, %. ΔP is the pressure difference, MPa. J_K is the permeability ratio of two tubes, decimal. V_{FA} is the total volume of injected foaming agents solution, PV. EOR_{KB} is the EOR of the tube with bigger permeability, %. EOR_{KS} is the EOR of the tube with smaller permeability, %.

The comparisions of the experimental results and the formulae (10) and (11) calculational results are depicted in Fig. 32 and Fig. 33. From Fig. 32 and Fig. 33, it can be seen that the calculational results can basically match the experimental results, which means formulae (10) and (11) can be applied to predict and study the air injection EOR effects in the heterogeneity reservoir formations.

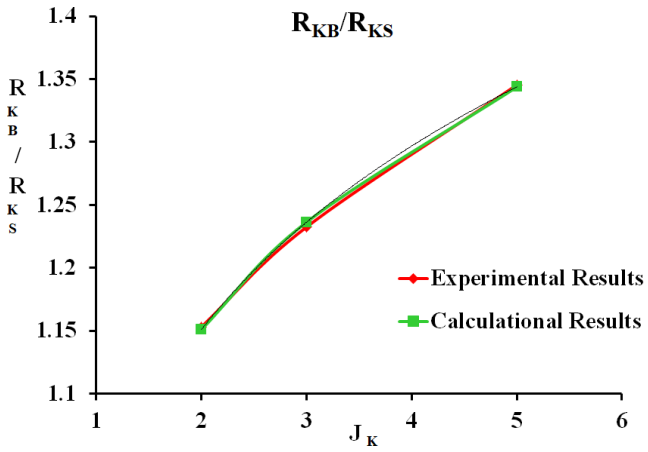

Fig. 32. The Final Recovery Factor Experimental and Calculational Results Comparison

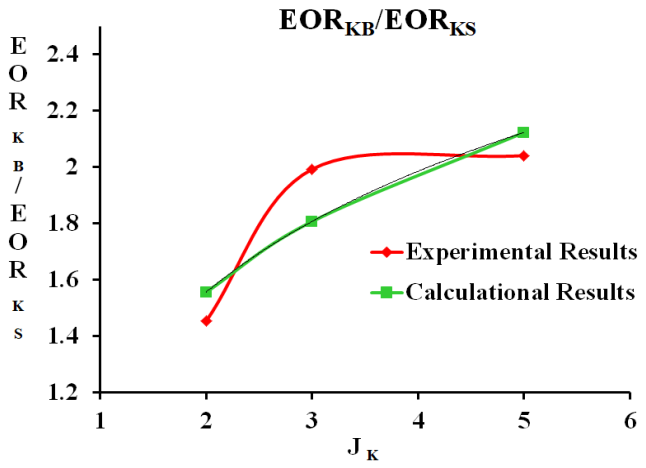

Fig. 33. The EOR Experimental and Calculational Results Comparison

5 Conclusion

The following conclusions can be made by analyzing the results of the experiments:

1. The best LTO effects can be gained by injecting deoxygenated air with 8% of oxygen into the target reservoir or reservoirs similar to it according to the studies. Moreover, the safety can be ensured because the oxygen concentration in the produced gas from the outlets was within the safety limits.
2. The best oxidation time was about 168 hours according to the experiments. However, when applied in the oil field production, this time period can be extended due to the existence of heterogeneity and the channeling tunnels according to the specific oil reservoir.
3. The best air injection rate was optimized as 0.3ml/min (7.41×10^{-4}PV/min) according to the EOR

results of the air injection period. This conclusion can be applied into the other similar oil field production after converting according to the reservoir parameters.

4. The higher the temperature was, the better the oil will be oxidized and the better the effects of the air flooding will be. However, the difference were not so obvious when the temperature was more than 105℃. So, the LTO effects under the initial condition was considered relatively good.
5. The recovery factor can be effectively enhanced by foam flooding.
6. The larger the permeability ratio was, the higher the EOR will be obtained by air-foam injection, especially in the formation which permeability ratio was larger.
7. Some formulae reveal the relationships of EOR and the parameters of the air injection and air-foam injection were deduced, which can provide some references for the study of the application of air injection technologies into some other similar low permeable oil reservoirs.

6 Acknowledgements

Our thanks are given to our fellow classmates and researchers of the same research team in carrying out the experiments. Finally, thanks for China University of Petroleum (Beijing) to provide the chance of carrying out this study and CNOOC to provide the oil and gas samples for the experiments.

References

[1] Guo, J., Li, Y., Zhao, J., Luo J. Numerical Simulation of Fracturing Naturally Fractured and Low-Permeability Reservoirs With Macro-Fracture. Petroleum Society of Canada. 2004, January 1. 1-6. https://doi:10.2118/2004-012.

[2] Greaves M., Ren S. R., Rathbone R.R.. Air Injection Technique (LTO Process) for IOR from Light Oil Reservoirs: Oxidation rate and displacement studies. SPE 40062, 1998: 479~492. https:// doi:10.2118/40062-MS.

[3] Sakthikumar, S., Madaoui, K., Chastang, J.. An Investigation Of The Feasibility Of Air Injection Into A Waterflooded Light Oil Reservoir. Society of Petroleum Engineers. January 1 1995; 343-356. https://doi:10.2118/29806-MS

[4] Turta, A. T., & Singhal, A. K. Reservoir Engineering Aspects of Oil Recovery from Low Permeability Reservoirs by Air Injection. Society of Petroleum Engineers. 1998, January 1. https://doi:10.2118/48841-MS

[5] Dongmei L., Michael. J., Intensive Production Enhancement of a Low-Permeability Oil Reservoir. Society of Petroleum Engineers; 2013. (SPE paper 168227) . https://doi:10.2118/168227-MS

[6] B. T. Hoffman, A. R. Kovscek, Light-Oil Steamdrive in Fractured Low-Permeability Reservoirs; 2003. (SPE paper 83491). https://doi:10.2118/83491-MS

[7] A. K. Alhuraishawy, B. J. Bai, M. Z. Wei, , et al., New Insights of Low Salinity Water Flooding in Low Permeability-Low Porosity Clay Rich Sandstone Reservoir; 2018. (SPE paper 193744). https://doi:10.2118/193744-MS

[8] T. A. Blasingame, The Characteristic Flow Behavior of Low-Permeability Reservoir Systems. Society of Petroleum Engineers; 2008 January 1. (SPE paper 114168). https:// doi:10.2118/114168-MS.

[9] A. T. Turta, A. K. Singhal, Reservoir Engineering Aspects of Oil Recovery from Low Permeability Reservoirs by Air Injection. Society of Petroleum Engineers; 1998 January 1. (SPE paper 48841). https://doi:10.2118/48841-MS.

[10] V. A. Baikov, A. Y. Davletbaev, D. S. Ivaschenko, Non-Darcy Flow Numerical Simulation and Pressure/Rate Transient Analysis for Ultra-Low Permeable Reservoirs; 2014. (SPE Paper 171174). https:// doi:10.2118/171174-MS.

[11] Shapour Vossoughl, Youssef EI-Shoubary, Kinetics of Crude-Oil Coke Combustion; SPE Reservoir Engineering, 1989; 201-106. https://doi:10.2118/16268-MS.

[12] M. Greaves, S. R. Ren, R. R. Rathbone, et al. Improved Residual Light Oil Recovery by Air Injection (LTO Process). JCPT 2000; 1: 57-61. https://doi:10.2118/169168-PA.

[13] M. R. Fassihi, R. G. Moore, S, A, Mehta et al., Safety Considerations for Air Injection into Light Oil Reservoirs; 2014. (SPE paper169168). https://doi:10.2118/169168-MS.

[14] Chu, C.. State-of-the-Art Review of Steamflood Field Projects. Society of Petroleum Engineers. (SPE paper 11733). 1985, October 1. https://doi:10.2118/11733-PA.

[15] D. Gutierrez, A. R. Taylor, H. V. K. Kumar, et al., Recovery Factors in High-Pressure Air Injection Projects Revisited; 2007. (SPE paper 108429). https://doi:10.2118/108429-PA.

[16] H. Rahnema, M. A. Barrufet, M., J. A. Martinez, et al. Dual Horizontal Well Air Injection Process. Society of Petroleum Engineers; 2012. (SPE Paper 153907). https:// doi:10.2118/153907-MS.

[17] T. Teranoto, H. Uematsu, K. Takabayashi, et al., Air Injection EOR in Highly Water Saturated Light-Oil Reservoir; 2006.(SPE paper 100215). https:// doi:10.2118/100215-MS.

[18] M. Greaves, S. R. Ren, T. X. Xia, New Air Injection Technology For IOR Operations In Light And Heavy Oil Reservoirs; 1999. (SPE paper 57295). https://doi:10.2118/57295-MS.

[19] Fassihi, M. R., Meyers, K. O., Baslie, P. F. Low-Temperature Oxidation of Viscous Crude Oils. Society of Petroleum Engineers. 1990 1: 609-616. https://doi:10.2118/15648-PA

[20] Gillham, T. H., Cerveny, B. W., Turek, E. A., et al,. Keys to Increasing Production Via Air Injection in Gulf Coast Light Oil Reservoirs; 1997. (SPE paper 38848). https://doi:10.2118/38848-MS.

[21] S. Bagci, D. Celebioglu, Light Oil Combustion With Metallic Additives in Limestone Medium. 55th Annual Technical Meeting. 2004. P. 1-12. https://doi:10.2118/2004-086.

[22] R. G. Moore, S. A. Mehta, M. G. Ursenbach, Potential for In-situ Combusiton in Depleted Conventional Oil Reservoirs; 2012. (SPE paper 154299). https://doi:10.2118/154299-MS.

[23] Teramoto, T., Uematsu, H., Takabayashi, K., Onishi, T.. Air Injection EOR in highly water saturated light-oil reservoir. Society of Petroleum Engineers. 2006, January 1. (SPE paper 100215). https://doi:10.2118/100215-MS.

[24] Ren, S. R., Greaves, M., Rathbone, R. R., Air Injection LTO Process: An IOR Technique for Light-Oil Reservoirs. SPE Journal 2002, 3: 90-99. https://doi:10.2118/57005-PA.

[25] Clara C., Durandeau M., Quenault G., et al., Laboratory Studies for Light-Oil Air Injection Projects: Potential Application in Handil Field; 1999. (SPE paper 54377). https:// doi:10.2118 /64272-PA.

[26] B. C. Watts, T. F. Hall, D. J. Petri, Horse Creek Air-Injection Project: An Overview. Society of Petroleum Engineers. Journal of Petroleum Technology 1998; 1: 78-80. https://doi:10.2118/383 59-MS.

[27] A.T. Turta, A.K. Singhal, Reservoir Engineering Aspects of Light-Oil Recovery by Air Injection; 1997. (SPE paper 38359). https://doi:10.2118/72503-PA.

[28] A. H. De Zwart, D. W. Van Batenburg, A. Tsolakidis, et al, The modeling challenge of high pressure air injection; 2008. (SPE paper 113917). https://doi:10.2118/113917-MS.

[29] M.G. Ursenbach, R.G. Moore, S.A. Mehta, Air Injection in Heavy Oil Reservoirs—A Process Whose Time Has Come (Again). Journal of Canadian Petroleum Technology 2003; 8: 39-45. https://doi:10.2118/132487-PA.

[30] Nazan N. Senol Topgüder, Laboratory Studies on Polymer Gels for CO_2 Mobility Control at Bat Raman Heavy Oilfield; 1999. (SPE paper 50798). https://doi:10.2118/50798-MS.

[31] Prabuddha Jain, Vinod Sharma, A.V. Raju, et al., Polymer Gel Squeeze for Gas Shutoff, Water

Shutoff and Injection Profile Improvement in Bombay High Pilot Wells; 2000. (SPE paper 64437). https://doi:10.2118/64437-MS.

[32] S. I. Chou, S. L. Vasicek, D. L. Pisio, CO2 Foam Field Trial at North Ward-Estes; 1992. (SPE paper 24643). https://doi:10.2118/24643-MS.

[33] Stanislav A. Zhdanov, A. V. Amiyan, Leonid M. Surguchev., Application of Foam for Gas and Water Shut-off: Review of Field Experience; 1996. (SPE paper 36914). https://doi:10.2118/36914-MS.

[34] S, I. Chou, CO_2 Foam Field Trial at North Ward-Estes; 1992. (SPE paper 24643). https://doi:10.2118/24643-MS.

[35] Tore Blaker, Morten Aarra, Arne Skauge, et al. Foam for Gas Mobility Control in the Snorre Field: The FAWAG Project; 1999. (SPE paper 78824). https://doi:10.2118/56478-MS.

[36] WANG B. J., LIANG J. Z., JIANG Y. W., et al. Foam Assisted Air Injection(FAAI) for IOR at Hailaer Oilfield: Prospects and challenges; 2013. (IPTC paper 16416). https://doi:10.2523/IPTC-16416-MS.

[37] A. Ocampo, A. Restrepo, H. Cifuentes, et al., Successful Foam EOR Pilot in a Mature Volatile Oil Reservoir Under Miscible Gas Injection; 2013. (IPTC paper 16984). https://doi:10.2523/IPTC-16984-MS.

[38] DAVID H. S. LAW, An Optimization Study For A Steam-Foam Drive Process In The Bodo Reservoir, Alberta". Journal of Canadian Petroleum Technology, 1992; 9: 33-40. https://doi:10.2118/92-09-04.

[39] P. C. LIU, Application of Foam Injection in Triassic Pool, Canada: Laboratory and Field Test Results; 1988. (SPE paper 18080). https:// doi:10.2118/18080-MS.

[40] W. T. OSTERLOH, M. J. JANTE, Effects of Gas and Liquid Velocity on Steady-State Foam Flow at High Temperature; 1992. (SPE paper 24179). https://doi:10.2118/24179-MS.

[41] L. CHENG, A. B. REME, D. SHAN, et al., Simulating Foam Processes at High and Low Foam Qualities; 2000. (SPE paper 59287). https://doi:10.2118/59287-MS.

[42] L. ROMERO-ZERON, A. KANTZAS, Pore Level Displacement Mechanisms During Foam Flooding; 2003. (Petroleum Society of Canada paper 2003-128). https://doi:10.2118/2003-128.